Hindawi
Advances in Materials Science and Engineering
Volume 2024, Article ID 5929170, 12 pages
https://doi.org/10.1155/2024/5929170

Research Article

Mechanical Behaviour of Glass Fibre-Reinforced Polymer/ Polyvinyl Chloride Foam Cored Sandwich Structures

Edwin Cheruiyot Kosgey,[1,2] **Krishnan Kanny**,[1] **and Festus Maina Mwangi**[1]

[1]*Mechanical Engineering Department, Durban University of Technology, Durban, South Africa*
[2]*Industrial and Energy Engineering Department, Egerton University, Nakuru, Kenya*

Correspondence should be addressed to Krishnan Kanny; kannyk@dut.ac.za

Received 23 January 2024; Revised 8 April 2024; Accepted 20 April 2024; Published 27 April 2024

Academic Editor: Murlidhar Patel

This study focuses on the fabrication and analysis of the mechanical behaviour of unidirectional (UD) glass fibre-reinforced polymer (GFRP) facesheet and polyvinyl chloride (PVC) foam core sandwich structures fabricated by a vacuum-assisted resin infusion method (VARIM). These sandwich structures are commonly used in marine and wind turbine blade applications. To date, relatively little knowledge about the functional behaviour of UD GFRP compared to composites reinforced with bidirectional mats is available for day-to-day applications. The effects of the facesheet orientation, facesheet thickness, and core thickness on the mechanical behaviour of the specimens were examined. The UD fibres were oriented in cross-ply (0/90), angle-ply (+45/−45), and quasi-isotropic orientations. Various mechanical properties such as tensile, flexural, flatwise compression, and edgewise compression tests were examined. Characterization of the tensile properties of the facesheet showed that the cross-ply orientation had a higher strength than the angle-ply and quasi-isotropic orientations. The flexural load-carrying capacity of the cross-ply facesheet orientation was superior to the other orientations. The increase in the core thickness changed the flexural failure mode from face yield and core shear to core indentation. Flatwise compression (FWC) was tested to determine the core characteristics of the sandwich structure, and the peak loads of 4.90, 1.81, and 3.90 kN were obtained for 10-, 15-, and 20 mm core thicknesses, respectively. Edgewise compression (EWC) exhibited stable end crushing for thinner facesheet, whereas thicker facesheet showed core crushing and buckling. When the facesheet thickness was increased from 1.5 mm to 3 mm in the EWC, the buckling load increase ranged from 2.53% to 44.83% for core thicknesses 10-, 15-, and 20 mm, respectively.

1. Introduction

Sandwich structures are constructed using cores surrounded by facesheets on both the sides [1–3]. The core has low density and light weight, whereas facesheets are stiff and thin and have high strength. The core contributes to the high specific bending stiffness of the sandwich structure and carries transverse shear loads, whereas the facesheets carry mainly tensile and compressive loads [4, 5]. The core materials used in marine environments (boats and yachts) and wind turbine blades include polyvinyl chloride (PVC), polyethylene terephthalate, and cardboard honeycomb, where PVC shows high energy absorption, high shear strength, and excellent bending properties [3]. Facesheets materials that are commonly used are glass fibre reinforced polymer (GFRP), carbon fibre reinforced polymer (CFRP), and natural fibres [6–8]. In sandwich structures, the damage induced is avoided by the arrangement of the plies in the interior section, thickness of the plies, and core thickness.

In recent years, many research studies have been conducted on the mechanical behaviour of sandwich structures under bending and compression conditions [1, 4, 9–22]. Polymer foams have been used as cores in sections exhibiting low shear properties. Foam cores can absorb a higher amount of energy before failure, owing to their improved toughness and ductility [23]. Modifications can be made in

the core by inducing a cut to improve shear strength and stiffness, but this may constitute a compromise on deflection [23]. The application of stiffeners between core and skins has been reported to decrease total deflection and improve shear resistance [24]. Density of the core in symmetrical and uniform configuration can improve the performance of flexural behaviour and energy absorption of sandwich structure [11, 14, 15]. Higher density core has tendency to increase flexural mechanical properties at lower resin uptake [9].

Core size is an important parameter that affects flexural performance and energy absorption sandwich structures [7, 13, 21]. Gupta et al. [13] studied the effect of different polyurethane core thicknesses of sandwich structures and plain weave glass fibre mat skins on flexural properties. An increase in core thickness contributed to a reduction in normal deflection, facial longitudinal stress, and core shear stress. The high core thickness contributed to a high moment of inertia, which increased the flexural strength and rigidity without adversely increasing the weight. Pandey et al. [7] studied the effect of core thickness on the flexural strength, energy absorption, and bending stiffness of carbon fibre facesheet and an aluminium foam core. The authors reported that the thickness of the hybrid foam core thickness increased the energy absorption and flexural properties of the sandwich structure. Similar results were reported by Xie et al. [1], where an increase in core thickness increased the stiffness and peak load by 44.7% and 60.5%, respectively. The core size alone is not sufficient to define the optimum design properties sandwich structures and should be combined with facesheet characteristics.

The fibre orientation and size of the facesheet have been reported to influence the mechanical behaviour of sandwich structures [18, 25, 26]. Mostafa et al. [18] studied the flexural response of PVC foam core and GFRP skins consisting of eight layers $(0, 90, 45, -45)_s$ of 2×2 twill weave E-glass. The authors reported that the sandwich panels failed with sudden brittle-type failure owing to shear failure of the core caused by debonding between the skin and the core. Rajanish et al. studied the influence of alumina nanoparticle on different angle of orientations of laminates [27]. Authors reported variations in shear properties for the different fibre orientations. Furthermore, the high value of unidirectional (UD) laminates originates from the 0° fibre orientation where the properties of the fibre are dominant because most of the load is taken up by fibres in that direction [27]. Xie et al. [1] studied the flexural properties of GFRP lattice web-reinforced polyethylene terephthalate (PET) foam sandwich panels. Authors reported that increasing facesheet thickness from 3.0 mm to 4.5 mm increased the ultimate load of the panel by 88.9%. Eyvasian et al. [26] reported that increasing the facesheet thickness increases the buckling load of the PVC foam core and dyneema/aluminium sandwich panels. A thinner facesheet leads to a smoother buckling phenomenon, implying that the core carries a compressive load compared to the facesheet.

The properties and strength of the foam core are important parameters that determine the collapse mode and crushing response of sandwich structure under edgewise compression [22]. Sandwich beams in the edgewise position exhibit high ultimate strength because of the presence of the fibre composite facesheet, whereas brittle-type failure occurs in the flatwise position of the beams [17]. The orientation of the facesheet layers in the flatwise compression of samples does not exhibit a significant variation in load, thus indicating a homogeneous flatwise characteristic [25]. Toygar et al. [28] studied the compression properties of sandwich structures with unsymmetrical face thickness of 3.75 mm and 1.4 mm. The authors reported that with the application of compressive force on the upper laminate with a thickness of 3.75 mm, the resultant shear stress between the upper laminate and core was 1.7 MPa and that between the lower laminate and core was 1.6 MPa. When the laminate thickness was changed to 1.4 mm, the shear stress obtained was 1.11 MPa and 1.13 MPa between the upper laminate and core and between the core and lower laminate, respectively. Lei et al. [29] studied the effect of slenderness ratio on edgewise compression of foam-filled sandwich structure. The authors reported that, with an increase in the slenderness ratio, the critical collapse strength of the column decreased, particularly for the same length.

The present experimental work on GFRP as facesheet is available in many engineering applications. However, little is known about the use of unidirectional GFRP arranged in different orientations and thicknesses for sandwich structures. There was limited literature where unidirectional GFRP has been oriented in different directions as a facesheet for sandwich structures compared to bidirectional mats. In this study, sandwich structures composed of different PVC foam core sizes and GFRP skins arranged in different orientations and stacking sequence mechanical responses were reported. The GFRP was arranged in cross-ply (0/90), angle-ply (+45/−45), quasi-isotropic, and bonded using an epoxy matrix via the vacuum resin infusion method (VARIM). The flexural behaviour, flatwise compression, and edgewise compression of the manufactured samples with different core thicknesses were determined experimentally. These sandwich panels are suitable for lightweight applications such as wind turbine blades, marine applications, and construction.

2. Materials and Experimental Methods

2.1. Materials. The sandwich structures used in this study comprised noncrimp glass fibres of 500 gsm and a PVC polymeric foam core. The fibres were arranged to form different stacking sequences and orientations, keeping ply numbers as four and eight layers to ensure a uniform facesheet thickness. Core thicknesses of 10-, 15-, and 20 mm with a density of 80 kg/m^3 were used. The technical material properties of the core obtained from the manufacturer are listed in Table 1. The chemicals used were LR30 epoxy resin and LH30 slow hardener mixed at a ratio of 100 : 25 by weight for resin to hardener. The LR30 epoxy resin and LH30 hardener have low viscosity and are suitable for the vacuum infusion process. The mixture is designed to exhibit excellent toughness and mechanical properties after post curing. The LH30 hardener has a pot life of 65 minutes and

curing time of 24–38 h. The tensile, compressive, and flexural strength of the mixture is 65, 120, and 131 MPa, respectively [30]. All materials and chemicals used were purchased from AMT composites, Durban.

2.2. Fabrication. The sandwich structure was fabricated using LR30 epoxy resin and LH30 hardener using the vacuum-assisted resin infusion method (VARIM) at pressures between 0 and 1.0 bar. The VARIM process is illustrated in Figure 1. First, the weight of the fibres was obtained using a digital weighing scale. Then, the required LR30 resin and LH30 slow hardener were calculated using the ratio 100 : 25 by weight of the fibres. The fibres were then laid in the mould with the core ready for infusion. Finally, LR30 and LH30 were mixed thoroughly in a glass beaker and placed at the suction point in the infusion assembly. The suction point was clamped when all mixtures were used. The assembly was left with the pump running for 24 h before demoulding.

The manufactured sandwich samples were post-processed in an oven with the maximum temperature maintained at 80°C for 4 h. The samples were produced as panels and cut using a band saw with a diamond blade to the required sizes, as per the relevant ASTM standard for each test. In the current study, samples containing cross-ply (0/90), angle-ply (+45/−45), and quasi-isotropic glass fibre-oriented facesheet and PVC foam cores of various thicknesses were marked for identification with notations and thickness sizes. For example, A20-4 means "A" for angle-ply orientation, "20" for core size (mm), and "4" to indicate 4 layers of plies. A similar notation was "C" for cross-ply and E represents quasi-isotropic.

2.3. Mechanical Testing

2.3.1. Tensile Test. Tensile tests of the fibre composite facesheet were performed following the ASTM D3039-00 standard [31]. The ends of the specimen were carefully clamped at the gripping area to avoid slippage which can result in premature failure. The specimens were tested at a test rate of 1 mm/min in tension using the MTS Criterion, Model 43, which is an electronic universal testing machine installed with a load cell capacity of 30 kN. The tensile stresses and strains were calculated based on the load and displacement data obtained from raw data. Three identical GFRP laminates were tested for each laminate category and the mean values were used for graphical illustration and discussion.

2.3.2. Flexural Test. The three-point bend (3PB) test was performed in a universal testing machine equipped with a 30 kN load cell at a crosshead speed of 3 mm/min. The 3PB test was performed according to ASTM C393-20 [32] with a standard span, L of 150 mm between the supports. Three identical specimens were tested for each sandwich panel, and the mean values were used to plot graphs and for discussion. The parameters b, d, t_f, and t_c represent width, mid-plane distance between core and facesheet, facesheet thickness, and core thickness of the specimens, respectively. The facesheet bending strength σ_f and core shear strength σ_{cs} were calculated using (1) [32] and (2) [32], respectively.

$$\sigma_f = \frac{F_{\max} \times L}{2t_f(d + t_c)b}, \tag{1}$$

$$\sigma_{cs} = \frac{F_{\max}}{(d + t_c)b}. \tag{2}$$

2.3.3. Compression Test. Flatwise and edgewise compression test was conducted using the MTS Criterion, Model 43, universal testing machine installed with a load cell capacity of 30 kN. The flatwise (FW) compression test was applied only to the 0/90 sample at a test rate of 1 mm/min. Since ASTM C365-03 [33] is core-dependent standard, one sample characteristic in FW was deemed sufficient to represent other samples. Edgewise compression (EW) test was carried out at a test rate of 1 mm/min according to ASTM C364-07 [34]. Three identical specimens were tested for each sandwich panel, and the mean values were used for analysis. The ultimate flatwise strength σ_{FW}^{ult}, flatwise compression modulus E_{FW}, and edgewise ultimate strength σ_{EW}^{ult} are indicated in (3) [35], (4) [35], and (5) [35], respectively. The other parameters, w, t_c, t_f, and t_t, represent the width, core thickness, facesheet thickness, and total sandwich thickness, respectively. Lastly, $F_{\max}$ and δ in FW corresponds to the maximum force matching to the maximum strain in compression of 2.0% and the respective displacement [35].

$$\sigma_{FW}^{ult} = \frac{F_{\max}}{A}, \tag{3}$$

$$E_{FW} = \frac{(F_{\max}/\delta) \times t_f}{A}, \tag{4}$$

$$\sigma_{EW}^{ult} = \frac{F_{\max}}{w(2t_f)}. \tag{5}$$

3. Results and Discussion

3.1. Tensile Properties of the Facesheet. Tensile testing of materials is used to determine the yield strength, proportional limit, elastic limit, and ultimate point. A stress-strain curve is plotted from normalized load-deflection data, and it is used to calculate the Young's modulus.

Figure 2 shows the typical stress-strain relationship of the GFRP facesheet laminate under tensile loading. The experimental results are listed in Table 2. It is necessary to characterize the tensile properties of GFRP laminates to determine their strength as facesheet in sandwich structures. The angle-ply A4 with 1.5 mm thickness GFRP had the lowest stress at 77.99 MPa, while cross-ply C4 was the highest at 396.36 MPa. The 3 mm quasi-isotropic laminate E8 had a stress value of 338.93 MPa and A8 had a stress value of 122.42 MPa. This phenomenon directly relates to the orientation of the glass fibre/epoxy laminate. The angle-ply

Table 1: PVC foam mechanical properties.

Density	Compressive strength	Compressive modulus	Shear strength	Shear modulus	Tensile strength	Tensile modulus
ASTM D1622	ASTM D1621-10	ASTM D1621-10	ASTM C 273	ASTM C273	ASTM D1623	ASTM D1623
80 kg/m^3	1.60 MPa	74 MPa	1.20 MPa	30 MPa	2.74 MPa	176 MPa

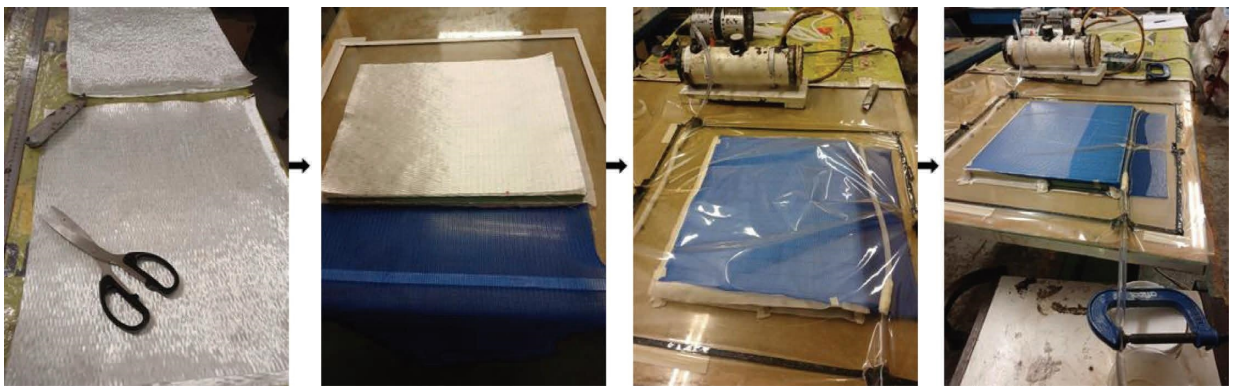

(a) (b) (c) (d)

Figure 1: Vacuum infusion process: (a) preparation of fibres, (b) laying of fibres in the mould, (c) complete setup of mould, and (d) infusion of epoxy resin.

orientation when subjected to tensile loading gives way to shear force, which results in multiple delamination in laminates followed by matrix cracking and then sudden fracture. At angle-ply orientation, the stress transfer between the fibre and the matrix is reduced owing to the less matrix content in the laminate which reduces the tensile strength [36]. The cross-ply laminates, C4 and C8, strength was high owing to the better strength that UD fibres offer in the longitudinal direction. Hence, cross-ply provides better control over the delamination and fracture loads than other orientations. Furthermore, the characteristics of the fibres deteriorate and are replaced by those of the matrix with change in fibre orientation [36, 37]. Similar results were reported by Das et al. [6] and Sing et al. [38] where 0° layup had highest tensile strength than other orientations.

Cross-ply C8 exhibited the highest Young's modulus of 17.60 GPa, followed by quasi-isotropic E8 at 10.32 GPa and lastly A8 at 2.84 GPa for 3.0 mm laminates. A similar trend was observed for 1.5 mm thick laminates. The Young's modulus was calculated from the linear portion of the stress-strain curves. An increase in fibre loading from 1.5 mm to 3 mm recorded an increase in the Young's modulus. Increasing the thickness implies an increase in the amount of fibre, which increases its tensile capabilities. From the experimental results obtained, the GFRP material exhibited good properties for the facesheet of a sandwich structure.

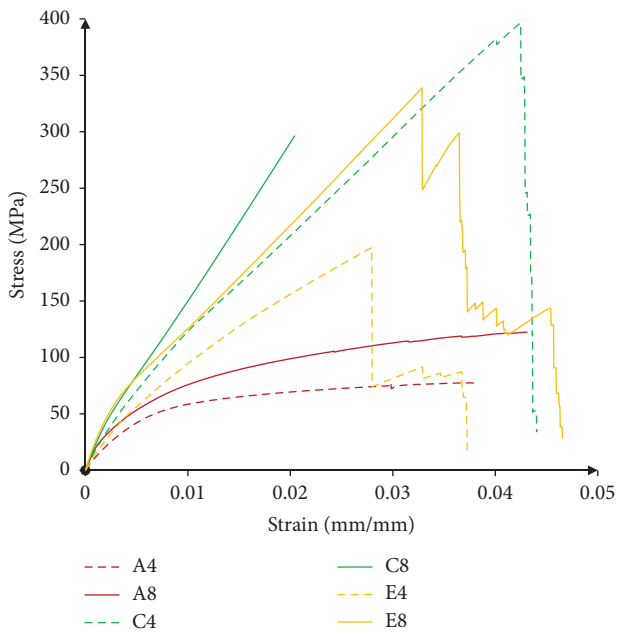

Figure 2: Stress versus strain curve for GFRP facesheet.

3.2. Flexural Response

3.2.1. Influence of Fibre Orientation. The load-displacement curves for 0/90, +45/-45, and quasi-isotropic GFRP-oriented PVC sandwich structures are shown in Figures 3–5 for 10-, 15-, and 20 mm core sizes, respectively. The failure modes that were observed in the experiments were face yield, core shear, face wrinkling, and indentation [1]. Independent of core size and face thickness, cross-ply orientation C20-4, C20-8, C15-4, C15-8, C10-4, and C10-8 exhibited the highest load-carrying capacity than other orientations.

The highest peak load was for C10-8 at 3.10 kN. The high load capacity of the cross-ply was due to the longitudinal direction of 0° unidirectional fibres, which provided resistance during loading [39]. This result was in agreement with the values obtained by Basturk [25], where 0/90 GFRP/PVC had an improved failure load/weight increase of 22% compared to the +45/−45 GFRP/PVC sample. The angle-ply

Table 2: Facesheet mechanical properties.

Test design	Young's modulus, E_f (GPa)	Yield strength, σ_f (MPa)
A4	2.62 ± 0.11	77.99 ± 1.36
C4	9.33 ± 0.18	396.36 ± 2.58
E4	7.07 ± 0.26	197.43 ± 5.91
A8	2.84 ± 0.09	122.42 ± 6.37
C8	17.60 ± 0.12	296.59 ± 8.14
E8	10.32 ± 0.35	338.93 ± 5.39

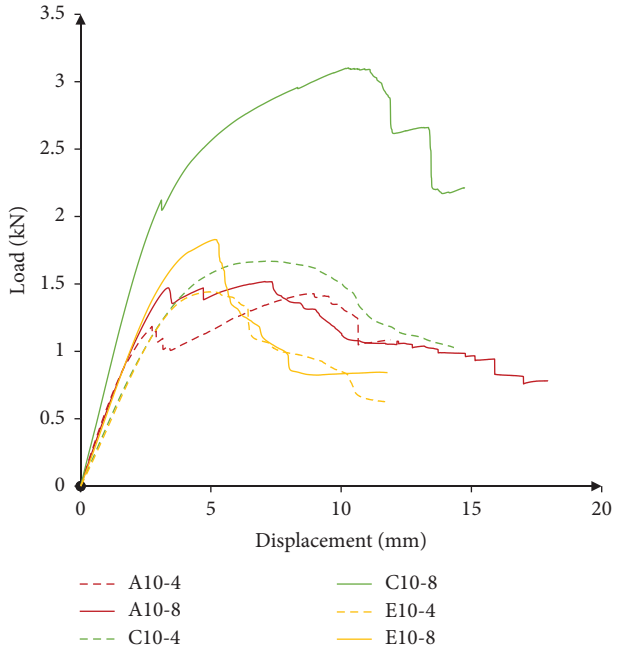

Figure 3: Load-deflection curves of 10 mm core size sandwich structures on 3PB.

orientation of the facesheet gave the lowest load-carrying capacity for all core thickness sizes. Liu et al. [2] reported similar superiority of unidirectional fibre arranged with 0° in longitudinal direction to the loading supports. For all the curves, a linear-elastic phenomenon was observed up to the peak point, followed by a decrease in loading due to failure that occurred in the sample. The formation of plateau in the curves is an indication of densification of core [40].

3.2.2. Influence of Facesheet Thickness. The facesheets in the samples were stacked in different layers, which gave approximate thickness of 1.5 mm and 3 mm, respectively. It is common knowledge that the top and bottom facesheets carry tensile and compressive loads, respectively [41]. Three failure modes are common in facesheets, i.e., face yield, face wrinkling, and indentation. As shown in Figures 3–5, the thicker facesheet carried more load than the thinner facesheet for all the core sizes. For a core size of 10 mm, thicker facesheet highest load carried was 3.104 kN,and the thinner facesheet carried 1.67 kN while the 15 mm core size carried the highest load of 2.87 kN for the thicker core and 1.38 kN

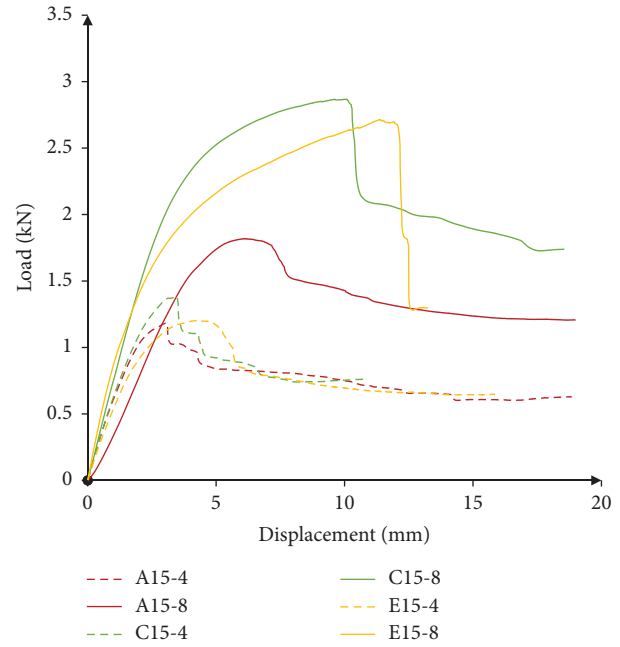

Figure 4: 3PB load versus deflection curve of 15 mm core sandwich structure.

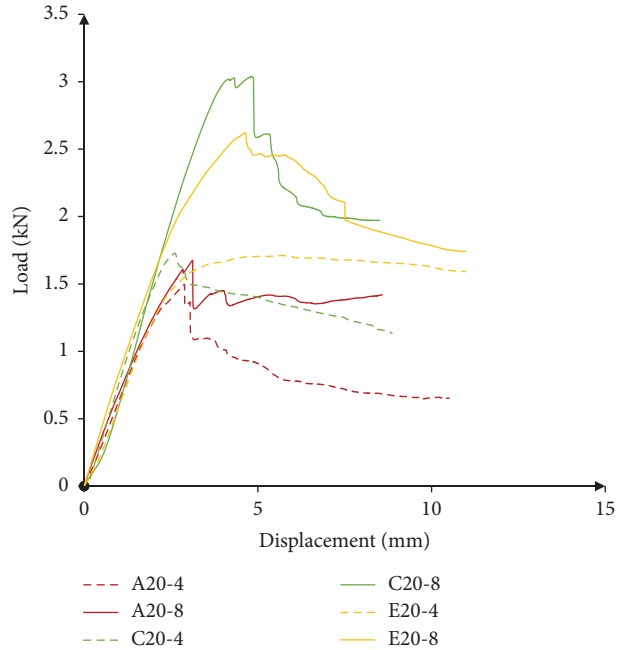

Figure 5: 3PB load-deflection curves of 20 mm core size sandwich structure.

for the thinner core. A thicker face size with a 20 mm core carried 3.04 kN and a thinner face size carried 1.79 kN. With an increase in the facesheet thickness from 1.5 mm to 3 mm, for the cross-ply orientation, the load carrying capacity increased by 46.20%, 58.74%, and 41.08% for 10-, 15-, and 20 mm core thickness, respectively. Similarly, for the angle-ply orientation, the load-carrying capacity increased by 5.94%, 34.92%, and 10.70% for 10-, 15-, and 20 mm core size,

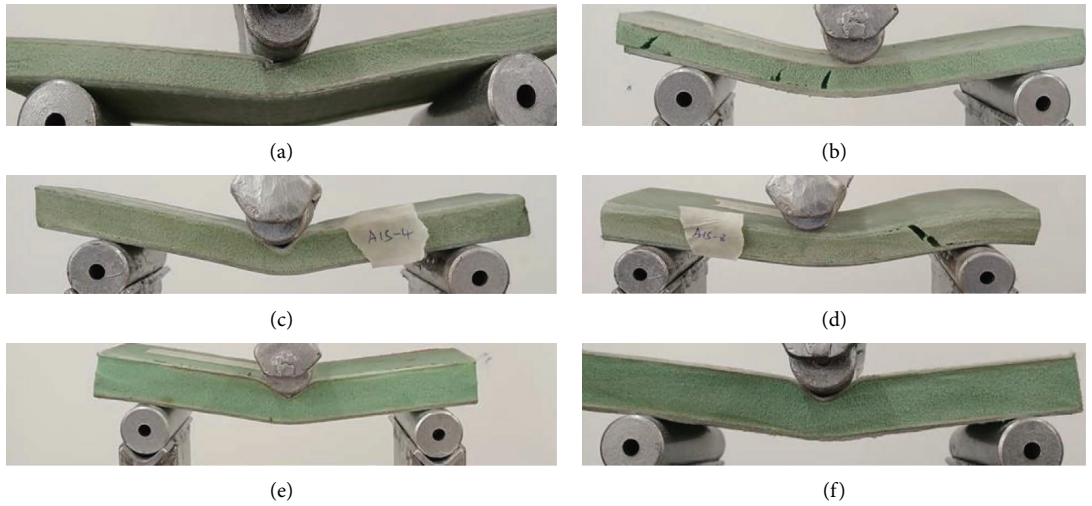

Figure 6: Damage modes of 3PB sandwich structures.

respectively. Finally, for the quasi-isotropic face orientation, the load-carrying capacity increased by 21.22%, 7.34%, and 34.71%, for the core sizes of 10-, 15-, and 20 mm, respectively. Each curve showed an initial linear elastic behaviour followed by a slowing down of the curve when approaching the peak load. The shapes of curves for the two facesheet thicknesses were similar. Visual observations revealed different failure mechanisms in the faces. The thinner core facesheet suffered facesheet failure in the cross-ply configuration and core shear as shown in Figures 6(a) and 6(b), respectively. The sandwich panel with a core size 15 mm suffered face indentation for a 1.5 mm facesheet and core shear for a 3 mm facesheet as shown in Figures 6(c) and 6(d). Figures 6(e) and 6(f) show the indentation damage on the core under load rollers for a 20 mm core size.

3.2.3. Influence of the Core Size. Previous studies have shown that the core carries shear loads [41] and energy absorption [42]. The typical load-displacement curves are shown in Figures 3–5. The curve increased linearly up to the peak load for each orientation curve. After the peak load, the stiffness decreased owing to the crack initiation in the core. As the thickness of the core increases, the slope and peak load also increase. From the damage assessment conducted, the specimen with a thinner core of 10 mm, shown in Figures 6(a) and 6(b), experienced core shear and face failure as the dominant failure mode. The panel for the 15 mm core size experienced face failure and core shear failure modes as shown in Figures 6(c) and 6(d). On the other hand, the specimen with a thicker core of 20 mm, shown in Figures 6(e) and 6(f), experienced indentation, and no observable core shear was noticed for all the tests conducted. Using the trapezoidal rule, the absorbed energy was calculated from the area enclosed in the load-deflection curves. The absorbed energy graph in Figure 7 shows that C10-8 had high energy absorption for all samples with a 10 mm core size, C15-8 for a 15 mm core size, and E20-4 for a 20 mm core size. Table 3 lists the absorbed energy and the corresponding peak loads of the sandwich structures.

3.3. Compression Characteristics

3.3.1. Flatwise Compressive Strength. A flatwise compression test of the sandwich structures was performed to determine the strength values and modulus under the loading direction normal to the facesheet [28]. Flatwise compression test is a core-dominated test [25], thus the results from the sample parameters used reflect the core characteristics.

Figure 8 shows the force-displacement curves (0/90) of the GFRP/PVC flatwise compression tests for the representative samples. The compressive strengths and moduli of the specimens are listed in Table 4. The foam-cored sandwich structures in the FWC exhibit different zones. The first zone (elastic zone) is a linear pattern in which the load increases linearly until it reaches a local maximum in a short period of time when the cells of the PVC foam start to collapse. The second zone (plateau phase) showed no variation in the load with time. The plateau phase is formed due to buckling and compaction of the PVC cell walls [25, 43]. The last section (densification phase) shows the force increases with a steep slope due to ending of collapse foams resulting in foam densification [25, 44].

3.3.2. Edgewise Compressive Strength. In edgewise compression (EWC), the force is applied in the axial direction of the sandwich facesheet. The failure mode in the EWC was determined using the ultimate edgewise compressive strength equation (28). The objective of the EWC test, as per results shown in Figures 9–11, was to obtain the edgewise compressive strength (σ_{EW}^{ult}) and compressive modulus of the GFRP/PVC sandwich structure. Furthermore, this study aimed to determine the contribution of the facesheet and core to the compressive strength and compressive modulus. All curves exhibited a linear curve up to the maximum load, followed by a reduction in the load. The EWC compression test is a facesheet dominated mode [26] and the damage modes are shown in Figure 12.

The maximum applied forces are presented in Table 4. The specimen with a thicker core exhibited a higher

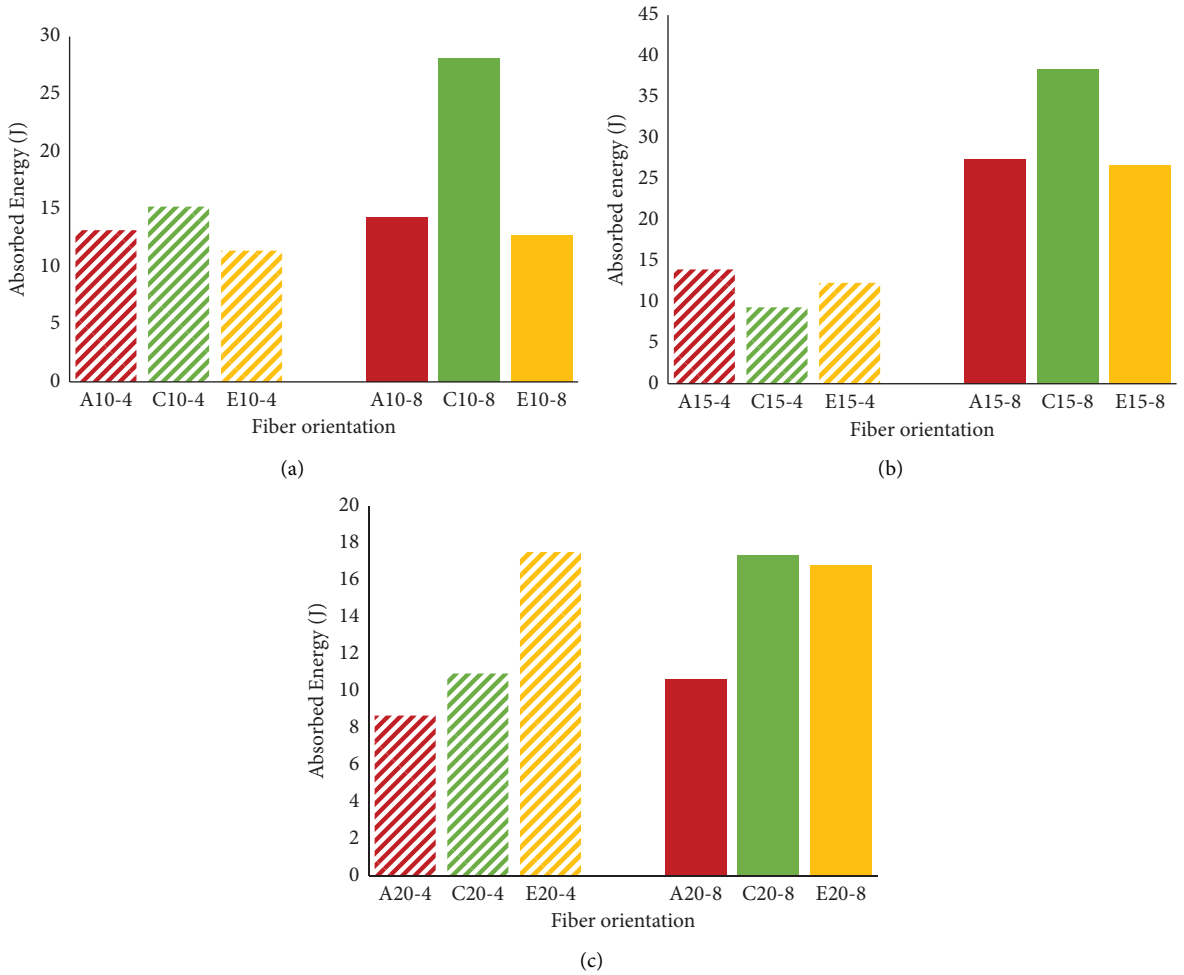

Figure 7: Absorbed energy: (a) 10 mm, (b) 15 mm, and (c) 20 mm core size of the sandwich structure under 3PB.

Table 3: Absorbed energy and peak load for sandwich panels on 3PB.

Specimen	Absorbed energy (J)	3PB peak load (kN)
A10-4	13.18	1.43 ± 0.13
A10-8	14.31	1.52 ± 0.35
C10-4	15.23	1.67 ± 0.09
C10-8	28.10	3.10 ± 0.61
E10-4	11.33	1.44 ± 0.55
E10-8	12.71	1.83 ± 0.20
A15-4	13.95	1.18 ± 0.16
A15-8	27.44	1.82 ± 0.04
C15-4	9.33	1.38 ± 0.38
C15-8	38.39	2.87 ± 0.19
E15-4	12.32	1.20 ± 0.11
E15-8	26.66	1.30 ± 0.37
A20-4	8.66	1.50 ± 0.21
A20-8	10.60	1.68 ± 0.08
C20-4	10.94	1.79 ± 0.24
C20-8	17.33	3.04 ± 0.63
E20-4	17.51	1.71 ± 0.49
E20-8	16.77	2.62 ± 0.14

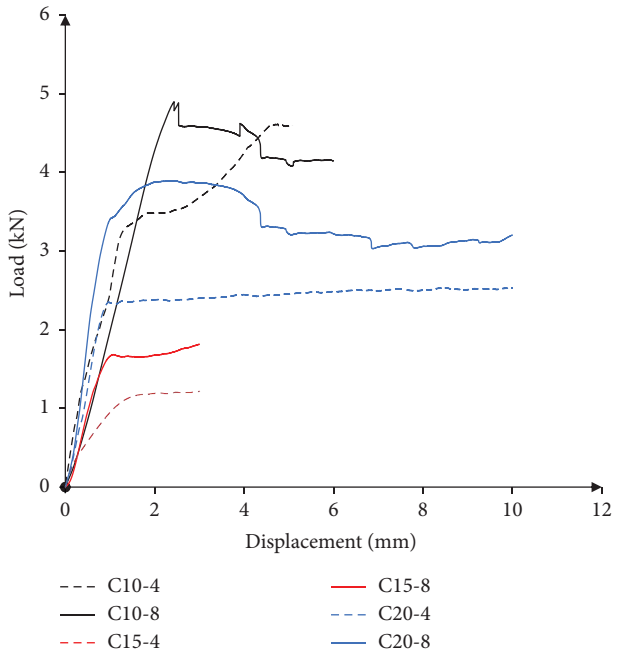

Figure 8: Flatwise compression tests of PVC foam core sandwich structures.

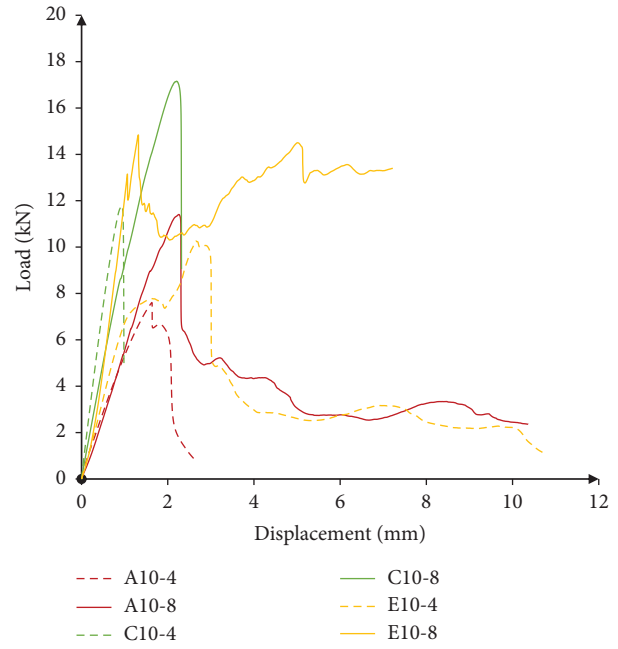

Figure 9: Edgewise compression of 10 mm core size sandwich structure.

Table 4: EW and FW compressive parameters.

Specimen	σ_{FW}^{ult} (MPa)	E_{FW} (MPa)	σ_{EW}^{ult} (MPa)	EWC peak load (kN)
A10-4	5.13	15.80	42.28	7.61 ± 0.54
A10-8	5.13	15.80	63.36	11.41 ± 0.89
C10-4	5.44	58.57	47.63	11.78 ± 0.74
C10-8	5.44	58.57	95.27	18.92 ± 1.13
E10-4	5.13	15.80	57.04	10.27 ± 0.83
E10-8	5.44	58.57	41.22	14.84 ± 0.71
A15-4	1.35	33.80	56.49	10.17 ± 0.70
A15-8	2.02	100.89	28.98	10.43 ± 0.96
C15-4	1.35	33.80	103.64	18.66 ± 0.63
C15-8	2.02	100.89	61.87	22.27 ± 1.25
E15-4	1.35	33.80	71.23	12.82 ± 1.28
E15-8	2.02	100.89	58.74	21.15 ± 1.17
A20-4	2.82	6.68	57.96	10.43 ± 1.12
A20-8	2.82	6.68	71.74	12.91 ± 0.56
C20-4	4.33	46.88	64.46	11.60 ± 0.88
C20-8	4.33	46.88	58.42	21.03 ± 0.98
E20-4	2.82	6.68	66.21	11.92 ± 1.56
E20-8	4.33	46.88	76.64	13.80 ± 1.92

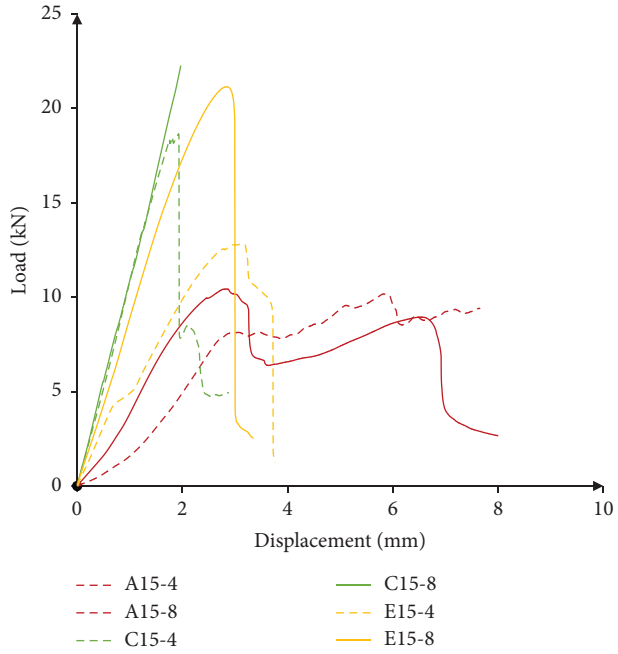

Figure 10: Edgewise compression of 15 mm core size sandwich structure.

compressive load than that with a low-thickness core. A sandwich panel with a thicker facesheet experienced failure between the core and skin, which can be linked to the shear force acting at the interfacial region. Specimens C10-8, C15-8, and C20-8 produced the largest critical failure load at 18.92, 22.27, and 21.03 kN for 10-, 15-, and 20 mm core sizes, respectively. When facesheet thickness was increased from 1.5 mm to 3 mm, for angle-ply orientation, the buckling load increased by 33.27%, 2.53%, and 19.21% for 10-, 15-, and 20-mm core thickness, respectively. For the cross-ply, it increased by 37.71%, 16.24%, and 44.83% for 10-, 15-, and 20 mm core thickness, respectively. Finally, for the quasi-isotropic orientation, the buckling load increased by 30.80%, 39.31%, and 13.62% for core thicknesses of 10-, 15-, and 20 mm, respectively. In the specimen with a thinner facesheet (1.5 mm), the buckling characteristic occurred more smoothly, which indicate the dominant effect of the PVC foam core in carrying compressive load when compared to the 3 mm facesheet. Furthermore, a thinner facesheet

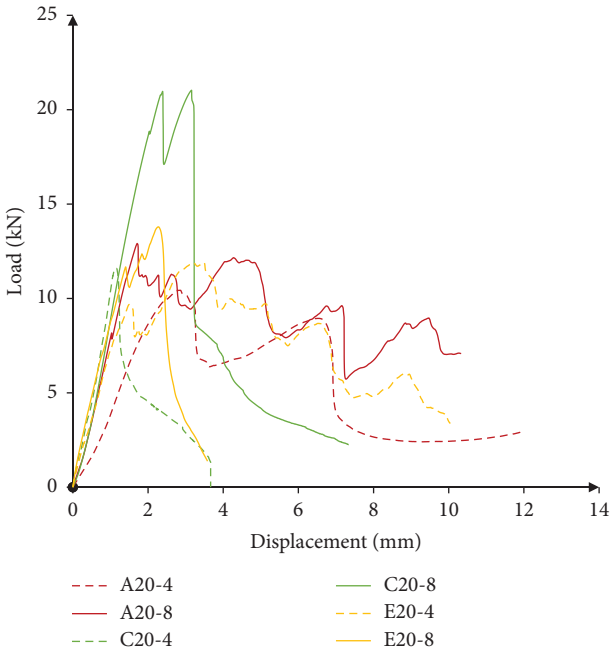

Figure 11: Edgewise compression of 20 mm core size sandwich structure.

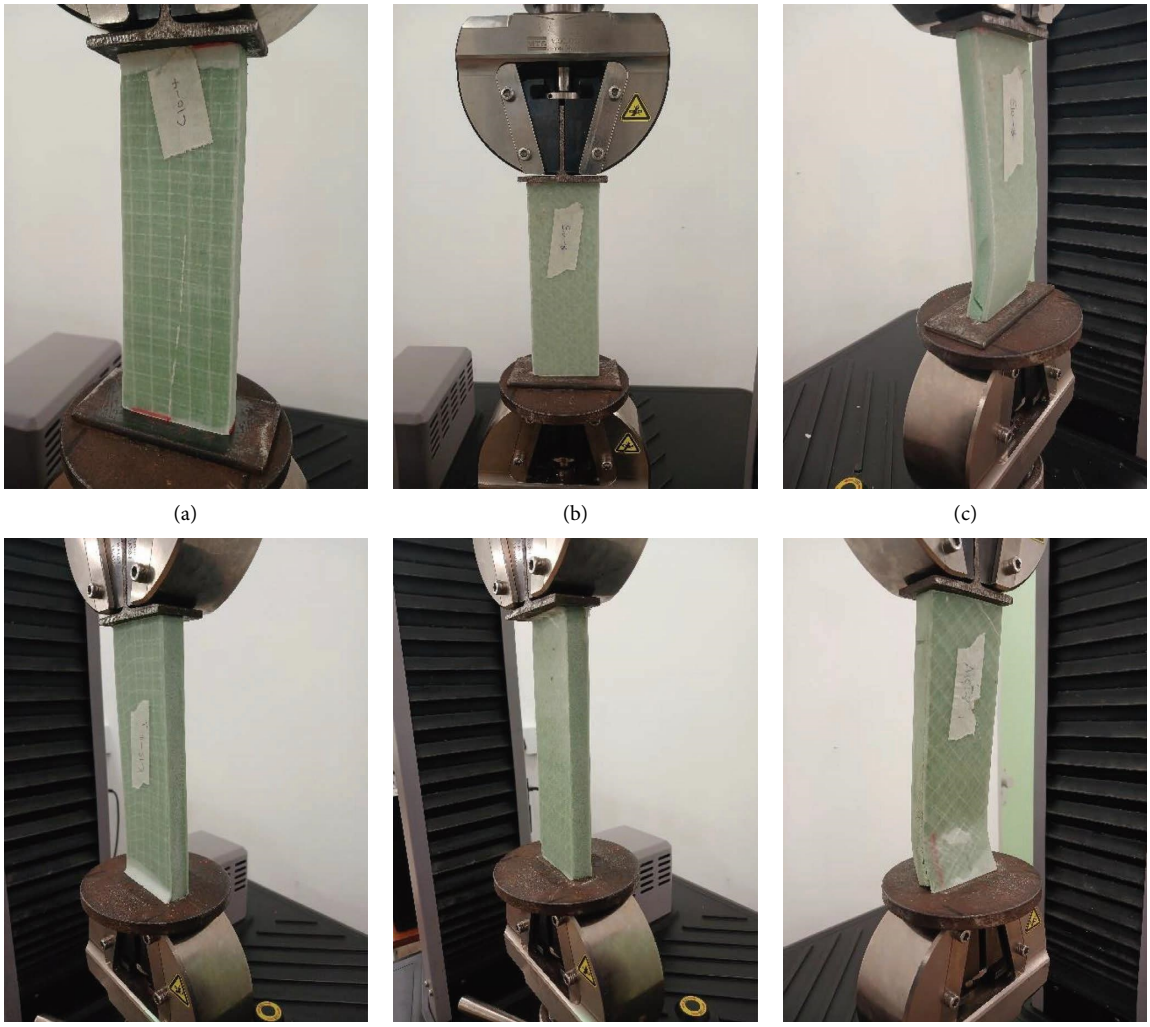

(a) (b) (c)

(d) (e) (f)

Figure 12: Continued.

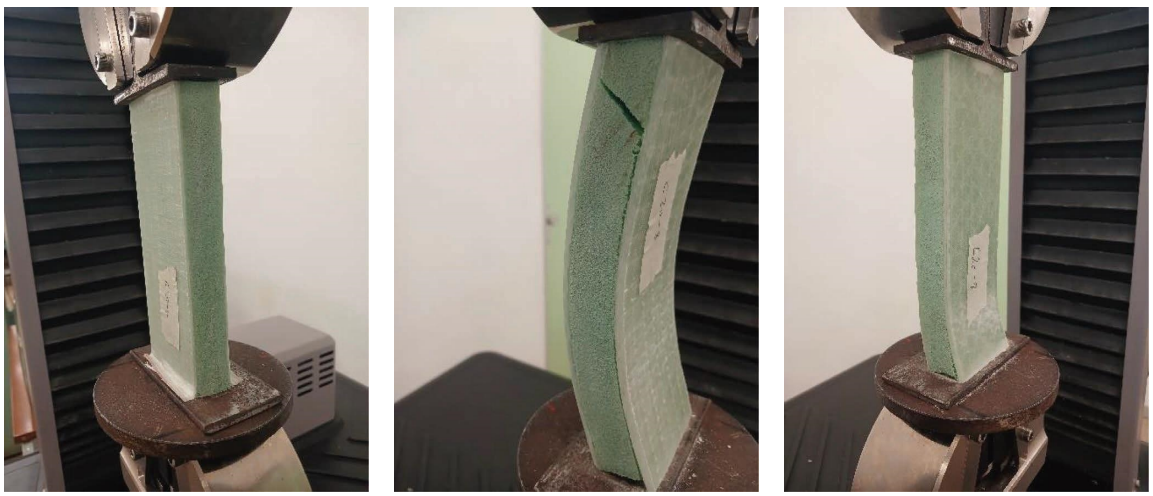

(g) (h) (i)

Figure 12: Damage mode of edgewise compression test.

sandwich panel developed end crushing and core densification, whereas a thicker facesheet led to stable buckling and core shear failure, as shown in Figure 12. A similar phenomenon was reported by Mamalis et al. [22], where the sandwich structure tended to collapse in three different modes as follows: mode I unstable, mode II unstable, and stable progressive end-crushing mode. The progressive end crushing mode is the most efficient mode for crash energy absorption and features several microcollapse mechanisms that aid in dissipating energy, increasing crushing load, and uniform compressive load distribution.

4. Conclusion

The GFRP/PVC foam sandwich structures were manufactured using a vacuum-assisted resin infusion method. The influence of the fibre orientation, facesheet size, and core size on the mechanical properties was investigated. The fibres were oriented to form cross-ply (0/90), angle-ply (+45/−45), and quasi-isotropic facesheet thickness of 1.5 mm and 3 mm were used. Core sizes of 10-, 15-, and 20 mm were investigated for flexural, flatwise, and edgewise compression properties. The results showed that C10-8, C15-8, and C20-8 had higher peak loads of 3.10, 2.87, and 3.04 kN, respectively, at 3PB. This high value for the cross-ply orientation was linked to the 0° longitudinal orientation of the fibres in the sample. The increase in the facesheet thickness from 1.5 mm to 3 mm increased the load-carrying capacity by 46.20%, 58.74%, and 41.08% for the cross-ply orientation; 5.94%, 34.92%, and 10.70% for the angle-ply orientation; and 21.22%, 7.34%, and 34.71% for the quasi-isotropic for 10-, 15-, and 20 mm core thickness, respectively. Damage assessment showed that thicker faces suffered face fracture as the dominant failure mode, and an increase in core size changed the failure mode from face failure to indentation.

Flatwise compression (FWC) was applied to cross-ply fibre orientation (0/90) for each face thickness and core size to represent other samples because it is a core-dominated mode. The highest FWC peak load was reported for 10 mm, followed by 20 mm and the lowest was for C15-4, 15 mm core size at 1 kN. In the edgewise compression test (EWC), the failure mode occurred as stable progressive end crushing for a 1.5 mm facesheet thickness for all core sizes, whereas thicker facesheet (3 mm) exhibited core shear and buckling. When facesheet thickness was increased from 1.5 mm to 3 mm in EWC, for angle-ply orientation, the buckling load increased by 33.27%, 2.53%, and 19.21%; for the cross-ply, the buckling load increased by 37.71%, 16.24%, and 44.83%, and lastly, for the quasi-isotropic orientation, the buckling load increased by 30.80%, 39.31%, and 13.62% for 10-, 15-, and 20 mm core thickness, respectively.

This study has possibility for more studies in quasistatic indentation and numerical simulation for comparison. Also, various failure modes can be represented using failure mode maps for prediction purposes. Furthermore, studies can be conducted to investigate the mechanical properties in dynamic loading conditions by low and high strain rates.

Data Availability

The data used to support the findings of this study are available from the corresponding author upon reasonable request.

Conflicts of Interest

The authors declare that they have no conflicts of interest.

Acknowledgments

The authors appreciate the support from the research office of Durban University of Technology by funding this research work. Open access funding was enabled and organized by SANLiC Gold.

References

[1] H. Xie, C. Shen, H. Fang, J. Han, and W. Cai, "Flexural property evaluation of web reinforced GFRP-PET foam

sandwich panel: experimental study and numerical simulation," *Composites Part B: Engineering*, vol. 234, 2022.

[2] J. Liu, Z. Dong, X. Zhu, W. Sun, and Z. Huang, "Flexural properties of lightweight carbon fiber/epoxy resin composite sandwiches with different fiber directions," *Materials Research Express*, vol. 9, no. 2, p. 026506, 2022.

[3] A. Robin, P. Davies, M. Arhant et al., "Mechanical performance of sandwich materials with reduced environmental impact for marine structures," *Journal of Sandwich Structures & Materials*, vol. 26, no. 2, pp. 99–113, 2024.

[4] S. Zhu, Y. Wang, L. Zhou et al., "Experimental investigation on mechanical behaviors of composite sandwich panels with a hybrid facesheet," *Polymer Composites*, vol. 44, no. 6, pp. 3196–3208, 2023.

[5] A. Russo and B. Zuccarello, "Experimental and numerical evaluation of the mechanical behaviour of GFRP sandwich panels," *Composite Structures*, vol. 81, no. 4, pp. 575–586, 2007.

[6] R. K. Das, B. Nayak, S. S. Gautam, and N. K. Rana, "Fabrication and characterisation of GFRP composite as skin material of sandwich structure," *Materials Today: Proceedings*, vol. 76, pp. 569–572, 2023.

[7] A. Pandey, D. Muchhala, R. Kumar, S. Sriram, A. C. Venkat, and D. Mondal, "Flexural deformation behavior of carbon fiber reinforced aluminium hybrid foam sandwich structure," *Composites Part B: Engineering*, vol. 183, 2020.

[8] A. A. Ajayi, M. Turup Pandurangan, and K. Kanny, "Influence of hybridizing fillers on mechanical properties of foam composite panel," *Polymer Engineering & Science*, vol. 63, no. 8, pp. 2565–2577, 2023.

[9] D. Cao, S. Malakooti, V. N. Kulkarni et al., "The effect of resin uptake on the flexural properties of compression molded sandwich composites," *Wind Energy*, vol. 25, no. 1, pp. 71–93, 2022.

[10] I. Daniel, E. Gdoutos, K. A. Wang, and J. Abot, "Failure modes of composite sandwich beams," *International Journal of Damage Mechanics*, vol. 11, no. 4, pp. 309–334, 2002.

[11] A. Farrokhabadi, S. Ahmad Taghizadeh, H. Madadi, H. Norouzi, and A. Ataei, "Experimental and numerical analysis of novel multi-layer sandwich panels under three point bending load," *Composite Structures*, vol. 250, 2020.

[12] N. Gupta, E. Woldesenbet, Kishore, and S. Sankaran, "Response of syntactic foam core sandwich structured composites to three-point bending," *Journal of Sandwich Structures & Materials*, vol. 4, no. 3, pp. 249–272, 2002.

[13] Y. Gupta, V. Paul V, A. Jacob, and A. Mohanty, "Effect of the core thickness on the flexural behaviour of polymer foam sandwich structures," *IOP SciNotes*, vol. 1, no. 2, 2020.

[14] C. Kaboglu, L. Yu, I. Mohagheghian, B. R. K. Blackman, A. J. Kinloch, and J. P. Dear, "Effects of the core density on the quasi-static flexural and ballistic performance of fibre-composite skin/foam-core sandwich structures," *Journal of Materials Science*, vol. 53, no. 24, Article ID 16393, 2018.

[15] M. Khan, A. Syed, H. Ijaz, and R. Shah, "Experimental and numerical analysis of flexural and impact behaviour of glass/pp sandwich panel for automotive structural applications," *Advanced Composite Materials*, vol. 27, no. 4, pp. 367–386, 2018.

[16] A. Khurram, M. A. Raza, P. Zhou, and T. Subhani, "A study of the nanocomposite sandwich structures for broadband microwave absorption and flexural strength," *Journal of Sandwich Structures & Materials*, vol. 18, no. 6, pp. 739–753, 2016.

[17] A. Manalo, T. Aravinthan, W. Karunasena, and M. Islam, "Flexural behaviour of structural fibre composite sandwich beams in flatwise and edgewise positions," *Composite Structures*, vol. 92, no. 4, pp. 984–995, 2010.

[18] A. Mostafa, K. Shankar, and E. Morozov, "Experimental, theoretical and numerical investigation of the flexural behaviour of the composite sandwich panels with PVC foam core," *Applied Composite Materials*, vol. 21, no. 4, pp. 661–675, 2014.

[19] A. Valenza, V. Fiore, and L. Calabrese, "Three-point flexural behaviour of GFRP sandwich composites: a failure map," *Advanced Composite Materials*, vol. 19, no. 1, pp. 79–90, 2010.

[20] H. Zniker, I. Feddal, B. Ouaki, and S. Bouzakraoui, "Experimental and numerical investigation of mechanical behavior and failure mechanisms of PVC foam sandwich and GRP laminated composites under three-point bending loading," *Journal of Failure Analysis and Prevention*, vol. 23, pp. 66–78, 2023.

[21] M. Ziaie, F. Zamani, S. Homayouni, H. Khaledi, A. Qareqani, and M. Ziaie, "Numerical and experimental study on mechanical properties of glass fiber-reinforced polymer sandwich structure with polyurethane foam-filled M-shaped core," *Polymer Composites*, vol. 44, no. 2, pp. 1054–1070, 2023.

[22] A. Mamalis, D. Manolakos, M. Ioannidis, and D. Papapostolou, "On the crushing response of composite sandwich panels subjected to edgewise compression: experimental," *Composite Structures*, vol. 71, no. 2, pp. 246–257, 2005.

[23] A. Fathi, F. Wolff-Fabris, V. Altstädt, and R. Gätzi, "An investigation on the flexural properties of balsa and polymer foam core sandwich structures: influence of core type and contour finishing options," *Journal of Sandwich Structures & Materials*, vol. 15, no. 5, pp. 487–508, 2013.

[24] J. Liu, J. Tao, F. Li, and Z. Zhao, "Flexural properties of a novel foam core sandwich structure reinforced by stiffeners," *Construction and Building Materials*, vol. 235, 2020.

[25] B. Baştürk, "Effect of fiber orientation on the mechanical properties of glass fiber reinforced polymer (GFRP)/PVC sandwich composites," *Karaelmas Fen ve Mühendislik Dergisi*, vol. 13, no. 1, pp. 52–61, 2023.

[26] A. Eyvazian, S. A. Taghizadeh, A. M. Hamouda, F. Tarlochan, M. Moeinifard, and M. Gobbi, "Buckling and crushing behavior of foam-core hybrid composite sandwich columns under quasi-static edgewise compression," *Journal of Sandwich Structures & Materials*, vol. 23, no. 7, pp. 2643–2670, 2021.

[27] M. Rajanish, N. Nanjundaradhya, and R. S. Sharma, "An investigation on ILSS properties of unidirectional glass fibre/alumina nanoparticles filled epoxy nanocomposite at different angles of fibre orientations," *Procedia Materials Science*, vol. 10, pp. 555–562, 2015.

[28] M. E. Toygar, K. F. Tee, F. K. Maleki, and A. C. Balaban, "Experimental, analytical and numerical study of mechanical properties and fracture energy for composite sandwich beams," *Journal of Sandwich Structures & Materials*, vol. 21, no. 3, pp. 1167–1189, 2019.

[29] H. Lei, K. Yao, W. Wen, H. Zhou, and D. Fang, "Experimental and numerical investigation on the crushing behavior of sandwich composite under edgewise compression loading," *Composites Part B: Engineering*, vol. 94, pp. 34–44, 2016.

[30] A. Composites, "Epoxy laminating resins LR30 and LH30 slow hardener," https://www.amtcomposites.co.za/wp-content/uploads/2021/06/LR-30.pdf.

[31] Astm, *Standard Test Method for Tensile Properties of Polymer Matrix Composite Materials*, ASTM International, West Conshohocken, PA, USA, 2000.

[32] Astm, *Standard Test Method for Core Shear Properties of Sandwich Constructions by Beam Flexure*, ASTM International, West Conshohocken, PA, USA, 2020.
[33] ASTM, *Standard Test Method For Flatwise Compressive Properties Of Sandwich Cores1*, ASTM International, West Conshohocken, PA, USA, 2003.
[34] ASTM, *Standard Test Method For Edgewise Compressive Strength Of Sandwich Constructions1*, ASTM International, West Conshohocken, PA, USA, 2007.
[35] R. Ferreira, D. Pereira, A. Gago, and J. Proença, "Experimental characterisation of cork agglomerate core sandwich panels for wall assemblies in buildings," *Journal of Building Engineering*, vol. 5, pp. 194–210, 2016.
[36] H. Sharath Chandra, K. Lokesh, G. Ravindra Babu, D. Shrinivasa Mayya, and J. Naveen Kumar, "Impact of fibre orientation on mechanical properties of GFRP composites," *Materials Today: Proceedings*, vol. 92, pp. 78–83, 2023.
[37] Y. S. Mohamed and A. Abdelbary, "Theoretical and experimental study on the influence of fiber orientation on the tensile properties of unidirectional carbon fiber/epoxy composite," *Alexandria Engineering Journal*, vol. 67, pp. 693–705, 2023.
[38] K. Singh and R. Shrivastava, "Influence of fiber orientation on thermo-mechanical response of symmetric glass/epoxy composite," *Journal of the Brazilian Society of Mechanical Sciences and Engineering*, vol. 45, no. 6, p. 288, 2023.
[39] R. O. Ogunleye, S. Rusnakova, M. Zaludek, and S. Emebu, "The influence of ply stacking sequence on mechanical properties of carbon/epoxy composite laminates," *Polymers*, vol. 14, no. 24, p. 5566, 2022.
[40] L. J. Gibson, "Cellular solids," *MRS Bulletin*, vol. 28, no. 4, pp. 270–274, 2003.
[41] F. Balıkoğlu and T. Demircioğlu, "Flexural behaviour of the composite sandwich beams with grid-scored foam: experimental and theoretical approach," *Thin-Walled Structures*, vol. 171, 2022.
[42] M. Kazemi, "Experimental analysis of sandwich composite beams under three-point bending with an emphasis on the layering effects of foam core," *Structures*, vol. 29, pp. 383–391, 2021.
[43] M. Mohamed, S. Anandan, Z. Huo, V. Birman, J. Volz, and K. Chandrashekhara, "Manufacturing and characterization of polyurethane based sandwich composite structures," *Composite Structures*, vol. 123, pp. 169–179, 2015.
[44] J. Mane, S. Chandra, S. Sharma et al., "Mechanical property evaluation of polyurethane foam under quasi-static and dynamic strain rates-an experimental study," *Procedia Engineering*, vol. 173, pp. 726–731, 2017.